Int. J. Solids Structures, 1970, Vol. 6, pp. 287 to 299. Pergamon Press. Printed in Great Britain

INTERACTION OF AN AXISYMMETRICALLY LOADED PLATE WITH THE ELASTIC SPACE

WILLIAM V. BREWER†

Department of Mechanical Engineering, University of Tulsa, Tulsa, Oklahoma

and

ROBERT WM. LITTLE

Department of Metallurgy, Mechanics and Materials Science, Michigan State University, East Lansing, Michigan

Abstract—The problem to be examined is that of a circular disk or plate attached to the wall of a cylindrical hole in an infinite solid. The interface boundary stress distribution will be compatible with simple plate theory and the slope and displacements are matched to the wall where the midplane of the plate intersects the solid. The problem is solved for any axisymmetric loading of a plate of uniform thickness and material parameters. This method can be easily extended to any axisymmetric plate solution without midplane forces. The material parameters in the plate and the supporting solid can be specified independently. In the specific examples included, plate deflections for a rigid wall assumption as opposed to a wall and plate of the same material never differ by less than 200%. There is little reason to believe that the trends indicated by the examples would change significantly for other usual loadings and geometries within the scope of the problem.

NOTATION

$A(\omega)$, $B(\omega)$	arbitrary coefficient functions of solutions to $\nabla^4\mathbf{Z}(r, z) = 0$
a, b	radius and half-thickness of the undeformed plate
c	$= 2(1-\nu)$ group of constants appearing frequently
D	$= \dfrac{2E_p b^3}{3(1-\nu_p^2)}$ plate modulus
E, ν	elastic material parameters
E_p, ν_p	elastic material parameters for the circular plate
E_W, ν_W	elastic material parameters for the wall supporting the plate
$\mathbf{F}$	vector potential function defined by Galerkin
G or G_W	$= \dfrac{E_W}{2(1+\nu_W)}$ elastic modulus in shear for the wall
$I_1(r)$	$= \displaystyle\int_0^r \frac{1}{\gamma}\int_0^\gamma \delta \int_0^\delta \frac{1}{\beta}\int_0^\beta \rho q(\rho)\,\mathrm{d}\rho\,\mathrm{d}\beta\,\mathrm{d}\delta\,\mathrm{d}\gamma$ an integral appearing in the general solution for the plate displacement $w(r)$
$I_2(r)$	$= \dfrac{\mathrm{d}}{\mathrm{d}r} I_1(r)$

† Formerly Graduate Research Assistant, Department of Mechanical Engineering, Michigan State University, East Lansing, Michigan.

$I_3(r)$ $= \frac{1}{r}\frac{d}{dr}(rI_2(r))$

$K_n(x)$ modified Bessel functions of the second kind and order n

$K(x)$ $= K_0(x)/K_1(x)$ group of terms appearing frequently

$M_r(r)$ moment resultant per unit circumferential length applied in the positive θ-direction (right-hand-rule) to the positive r-face of a differential element of plate material $(dr) \times (r\,d\theta) \times (2h)$

$Q_r(r)$ shear resultant per unit circumferential length applied in the positive z-direction to the positive r-face of a differential element of plate material $(dr) \times (r\,d\theta) \times (2h)$

$q(r)$ plate load per unit area applied in the positive z-direction to the z-face of a differential element of plate material $(dr) \times (r\,d\theta) \times (2h)$

(r, θ, z) cylindrical coordinates

S maximum σ_r on the common boundary between the plate and the supporting wall

T maximum τ_{rz} on the common boundary between the plate and the supporting wall

$ss(r, z)$, $st(r, z)$, $ts(r, z)$, $tt(r, z)$, $us(r, z)$, $ut(r, z)$, $uzs(r, z)$, $uzt(r, z)$, $ws(r, z)$, $wt(r, z)$ infinite integrals appearing in the displacement solution of the elastic solid

$\mathbf{u}$ $= (u_r, v_\theta, w)$ displacement vector in the elastic solid

$u_r(r, z)$ displacement of the elastic solid in the r-direction

v_θ $= 0$ displacement of the elastic solid in the θ direction

$w(r)$ displacement of the plate in the z-direction

$w(r, z)$ displacement of the elastic solid in the z-direction

$Z(r, z)$ component of Galerkin's vector potential $\mathbf{F}$ in the z-direction . . also referred to as the Love strain function

$\phi(x)$ $= \frac{\sin(x)}{x} - \cos(x)$ and $\psi(x) = x^2(K^2(x) - 1) - c$ are groups of terms appearing frequently in the displacement solutions

$\sigma_r, \sigma_\theta, \sigma_z$, etc. tensile stress in the indicated directions

$\tau_{rz}, \tau_{r\theta}, \tau_{\theta z}$ shear stress on the faces and in the directions indicated where $\tau_{ij} = \tau_{ji}$ for all cases considered

ω separation parameter in the solution of $\nabla^4 Z = 0$

1. INTRODUCTION

IT IS easily recognized that the elasticity of a solid supporting wall may contribute significantly to the deflections of the thin member which is attached to it. The assumption that the wall is rigid may lead to sizeable errors depending upon the relative material properties of the wall and the member. The interaction problems of beams and plates with supporting walls are the most common in practice and the beam problem has received considerable attention in the past. The problem is usually modeled in the plane elasticity sense either by plane stress or plane strain, and is considered as interacting with the elastic half-plane. This problem has been investigated independently by Weber [1] and Muskhelishvili [2], each employing different boundary conditions at the interface. Weber modeled the problem by applying to the half-plane the linear axial tensile stress distribution obtained by simple beam theory. Muskhelishvili, however, applied a linear axial displacement condition at the interface. O'Donnell [3] compared these solutions and noted that the displacements due to the rotation differed by only 15% even though the stress in the case of the displacement condition is infinite at the edge. O'Donnell chose a cubic stress distribution as a more realistic condition and obtained results between the other two. He also investigated the effect of shear by applying a constant shear to the wall and experimentally verified these results.

More recently, Cook [4] generalized the plane-stress beam problem to infinitely many evenly spaced cantilever beams intersecting a supporting beam. Each beam was loaded

with the same moment and the problem was solved numerically by the finite-element method for a range of relevant dimensional ratios.

An investigation of the non-plane intersection problem of a shaft of circular cross-section with the half-space has been conducted by Brown and Hall [5]. The axial tensile stress from simple beam theory is applied at the interface and the deflections are obtained and compared with experimental results. The effects of shear stresses were not considered in this investigation.

2. FORMULATION OF THE PROBLEM

The problem to be investigated here is that of a circular disk or plate attached to the wall of a cylindrical hole in an infinite solid. Only axially-symmetric loadings will be considered so that the dependency upon the angle may be ignored. The disk and the shaft will share the same axis of symmetry, the z axis. The undeformed disk will occupy the space $-b \leq z \leq +b$ and $0 \leq r \leq a$. The elastic space will be described by classical three-dimensional elasticity theory for an isotropic homogeneous medium.

The problem of a shaft in an infinite solid has been treated for several simple loadings: semi-infinite hydrostatic pressure [6]; localized hydrostatic pressure [7]; localized shear [8]. More recently Blenkarn and Wilhoit [9] applied a localized hydrostatic pressure to the entrance of a hole in a semi-infinite solid.

Plate theory will be used for the disk and the effect of the midplane forces in the disk will be ignored.

The interface boundary conditions will be compatible to the stress distribution of simple plate theory and are as follows:

$$\sigma_r(r = a, -b \leq z \leq b) = Sz/b \tag{1}$$

$$\tau_{rz}(r = a, -b \leq z \leq b) = T(1-z^2/b^2) \tag{2}$$

where S and T are constants to be determined by the loading on the plate.

Since only the stresses are specified at the interface and the displacement conditions will have to be approximated, we will expect errors in the local area of the interface. Based upon Saint Venant's Principle and O'Donnell's findings, we do not expect the gross deflections of the plate to be greatly altered by this assumption.

3. INFINITE SOLID

The Navier equation for the elasto-static problem without body forces is

$$\nabla^2\mathbf{u} + \frac{1}{1-2\nu}\nabla(\nabla \cdot \mathbf{u}) = 0. \tag{3}$$

Using the Galerkin vector defined as follows

$$2G\mathbf{u} = 2(1-\nu)\nabla^2\mathbf{F} - \nabla(\nabla \cdot \mathbf{F}) \tag{4}$$

the Navier equation reduces to a biharmonic vector equation in terms of the Galerkin vector.

$$\nabla^2\nabla^2\mathbf{F} = 0. \tag{5}$$

For the case of axial symmetry, only the z-component of the Galerkin vector is needed which is known as the Love strain function.

$$\mathbf{F} = [0, 0, Z(r, z)]. \tag{6}$$

The displacements and stresses may be expressed in terms of Z as follows:

$$\begin{aligned}
2Gw &= \left[2(1-\nu)\nabla^2 - \frac{\partial^2}{\partial z^2}\right]Z \\
2Gv_\theta &= 0 \\
2Gu_r &= -\frac{\partial^2 Z}{\partial r \partial z} \\
\sigma_z &= \frac{\partial}{\partial z}\left[(2-\nu)\nabla^2 - \frac{\partial^2}{\partial z^2}\right]Z \\
\sigma_r &= \frac{\partial}{\partial z}\left(\nu\nabla^2 - \frac{\partial^2}{\partial r^2}\right)Z \\
\sigma_\theta &= \frac{\partial}{\partial z}\left(\nu\nabla^2 - \frac{1}{r}\frac{\partial}{\partial r}\right)Z \\
\tau_{rz} &= \frac{\partial}{\partial r}\left[(1-\nu)\nabla^2 - \frac{\partial^2}{\partial z^2}\right]Z \\
\tau_{r\theta} &= \tau_{\theta z} = 0.
\end{aligned} \tag{7}$$

Noting that the boundary conditions imply that only the even functions in z need to be considered, the solution of the biharmonic equation for Z may be taken in the form

$$Z = \int_0^\infty \sqrt{\left(\frac{2}{\pi}\right)} \frac{1}{\omega^2}\left[A(\omega)K_0(\omega r) + B(\omega)\omega r K_1(\omega r)\right]\cos(\omega z)\,d\omega \tag{8}$$

where $K_0(\omega r)$ and $K_1(\omega r)$ are the modified Bessel functions of the second kind. This solution exhibits the property that it decays as r approaches infinity and is even in z.

The interface boundary conditions, equations (1) and (2), take the form

$$\begin{aligned}
&\int_0^\infty \sqrt{\left(\frac{2}{\pi}\right)}\left[A(\omega)\left(K_0(\omega a) + \frac{1}{\omega a}K_1(\omega a)\right) - B(\omega)\left([1-2\nu]K_0(\omega a) - \omega a K_1(\omega a)\right)\right]\sin(\omega z)\,d\omega \\
&\quad = \begin{cases} S\,z/b & -b \le z \le +b \\ 0 & -b > z > b \end{cases} \\
&\int_0^\infty \sqrt{\left(\frac{2}{\pi}\right)}\left[-A(\omega)K_1(\omega a) + B(\omega)\left(2[1-\nu]K_1(\omega a) - \omega a K_0(\omega a)\right)\right]\cos(\omega z)\,d\omega \\
&\quad = \begin{cases} T(1-z^2/b^2) & -b \le z \le b \\ 0 & -b > z > b \end{cases}
\end{aligned} \tag{9}$$

These two equations may be solved for the unknown functions $A(\omega)$ and $B(\omega)$ by use of the Fourier sine and cosine transforms

$$f(\omega) = \int_0^\infty \sqrt{\left(\frac{2}{\pi}\right)} F_s(z) \sin(\omega z)\, dz$$
$$g(\omega) = \int_0^\infty \sqrt{\left(\frac{2}{\pi}\right)} G_c(z) \cos(\omega z)\, dz. \tag{10}$$

The functions A and B become

$$A(\omega) = \sqrt{\left(\frac{2}{\pi}\right)} \frac{\phi(\omega b)}{\psi(\omega a) K_1(\omega a)} \left[Sa\left(\omega a K(\omega a) - c\right) + \frac{2\,Ta}{\omega^2 ab}\left(\omega^2 a^2 - (c-1)\omega a K(\omega a)\right)\right]$$
$$B(\omega) = -\sqrt{\left(\frac{2}{\pi}\right)} \frac{\phi(\omega b)}{\psi(\omega a) K_1(\omega a)} \left[Sa + \frac{2\,Ta}{\omega^2 ab}\left(1 + \omega a K(\omega a)\right)\right] \tag{11}$$

where use has been made of the symbols

$$K(x) = \frac{K_0(x)}{K_1(x)} \qquad \phi(x) = \frac{\sin(x)}{x} - \cos(x)$$
$$c = 2(1-\nu)$$
$$\psi(x) = [x^2(K^2(x) - 1) - c]$$

to simplify the notation.

When expressions (11) for $A(\omega)$ and $B(\omega)$ are substituted into the strain function (8) and it in turn is substituted into the general expressions (7), the resulting equations (12) shown below are valid everywhere in the elastic solid.

$$Gw(r, z) = S\left\{\frac{a}{\pi}\int_0^\infty \frac{\phi(\omega b) K_1(\omega r)}{\omega \psi(\omega a) K_1(\omega a)} \left[\left(\omega a K(\omega a) + c\right) K(\omega r) - \omega r\right] \cos(\omega z)\, d\omega\right\}$$
$$+ T\left\{\frac{2}{\pi b}\int_0^\infty \frac{\phi(\omega b) K_1(\omega r)}{\omega^3 \psi(\omega a) K_1(\omega a)} \left[\left(\omega^2 a^2 - (c-1)\omega a K(\omega a)\right) K(\omega r)\right.\right.$$
$$\left.\left. - \left(1 + \omega a K(\omega a)\right)\left(\omega r - 2c K(\omega r)\right)\right] \cos(\omega z)\, d\omega\right\}$$
$$Gu_r(r, z) = S\left\{\frac{-a}{\pi}\int_0^\infty \frac{\phi(\omega b) K_1(\omega r)}{\omega \psi(\omega a) K_1(\omega a)} \left[\left(\omega a K(\omega a) - c\right) - \omega r K(\omega r)\right] \sin(\omega z)\, d\omega\right\}$$
$$+ T\left\{\frac{-2}{\pi b}\int_0^\infty \frac{\phi(\omega b) K_1(\omega r)}{\omega^3 \psi(\omega a) K_1(\omega a)} \left[\left(\omega^2 a^2 - (c-1)\omega a K(\omega a)\right)\right.\right.$$
$$\left.\left. - \left(1 + \omega a K(\omega a)\right)\omega r K(\omega r)\right] \sin(\omega z)\, d\omega\right\}$$

$$
\begin{aligned}
G\frac{\partial u_r}{\partial z}(r,z) &= S\left\{\frac{-a}{\pi}\int_0^\infty \frac{\phi(\omega b)K_1(\omega r)}{\psi(\omega a)K_1(\omega a)}\left[\left(\omega aK(\omega a-c\right)-\omega rK(\omega r)\right]\cos(\omega z)\,d\omega\right\}\\
&\quad + T\left\{\frac{-2}{\pi b}\int_0^\infty \frac{\phi(\omega b)K_1(\omega r)}{\omega^2\psi(\omega a)K_1(\omega a)}\left[\left(\omega^2a^2-(c-1)\omega aK(\omega a)\right)\right.\right.\\
&\quad \left.\left.-\left(1+\omega aK(\omega a)\right)\omega rK(\omega r)\right]\cos(\omega z)\,d\omega\right\}\\
\sigma_r(r,z) &= S\left\{\frac{2a}{\pi}\int_0^\infty \frac{\phi(\omega b)K_1(\omega r)}{\psi(\omega a)K_1(\omega a)}\left[\left(\omega aK(\omega a)\right)\left(K(\omega r)+\frac{1}{\omega r}\right)-\left(K(\omega r)+\omega r+\frac{c}{\omega r}\right)\right]\right.\\
&\quad \left.\sin(\omega z)\,d\omega\right\}\\
&\quad + T\left\{\frac{4}{\pi b}\int_0^\infty \frac{\phi(\omega b)K_1(\omega r)}{\omega^2\psi(\omega a)K_1(\omega a)}\left[\left(\omega^2a^2-(c-1)\omega aK(\omega a)\right)\left(K(\omega r)+\frac{1}{\omega r}\right)\right.\right.\\
&\quad \left.\left.+\left(1+\omega aK(\omega a)\right)\left((c-1)K(\omega r)-\omega r\right)\right]\sin(\omega z)\,d\omega\right\}\\
\tau_{rz}(r,z) &= S\left\{\frac{-2a}{\pi}\int_0^\infty \frac{\phi(\omega b)K_1(\omega r)}{\psi(\omega a)K_1(\omega a)}\left[\omega aK(\omega a)-\omega rK(\omega r)\right]\cos(\omega z)\,d\omega\right\}\\
&\quad + T\left\{\frac{-4}{\pi b}\int_0^\infty \frac{\phi(\omega b)K_1(\omega r)}{\omega^2\psi(\omega a)K_1(\omega a)}\left[\left(\omega^2a^2-(c-1)\omega aK(\omega a)\right)\right.\right.\\
&\quad \left.\left.+\left(1+\omega aK(\omega a)\right)\left(c-\omega rK(\omega r)\right)\right]\cos(\omega z)\,d\omega\right\}.
\end{aligned}
\tag{12}
$$

The integral quantities in the braces of equations (12) will be designated as indicated below and are computed with the aid of a CDC 3600 digital computer.

$$
\begin{aligned}
Gw(r,z) &= S\{ws(r,z)\}+T\{wt(r,z)\}\\
Gu_r(r,z) &= S\{us(r,z)\}+T\{ut(r,z)\}\\
G\frac{\partial u_r}{\partial z}(r,z) &= S\{uzs(r,z)\}+T\{uzt(r,z)\}\\
\sigma_r(r,z) &= S\{ss(r,z)\}+T\{st(r,z)\}\\
\tau_{rz}(r,z) &= S\{ts(r,z)\}+T\{tt(r,z)\}
\end{aligned}
\tag{13}
$$

A suitable numerical integration procedure was obtained from the Euler–MacLauren summation formula [10]. The integrals have decaying periodic behavior owing to the dominance of sinusoidal elements for large values of ω. It was noted that the successive partial sums approximating the integral will exhibit maxima and minima for sufficiently small intervals and that these values bound the desired value of the infinite integrals. As the b/a ratio approaches zero, the numerical complexities of the problem increase greatly.

3. CIRCULAR PLATE

The circular plate will be subjected to any axisymmetrical loading consistent with the assumptions made so far in this development. The in-plane displacements will be considered to be negligible and elementary plate theory will be used in the development. The interface boundary conditions are obtained from matching the deflections and slopes of the midplane of the plate to the appropriate deflections and slopes from the elastic solid and may be stated as follows:

	Plate		Elastic solid
(a)	$w(a)$	=	$w(a, 0)$
(b)	$\dfrac{\mathrm{d}w(a)}{\mathrm{d}r}$	=	$-\dfrac{\partial u}{\partial z}(a, 0)$
(c)	$M_r(a)$	=	$\int \sigma_z(a, z)z \, \mathrm{d}A$
(d)	$Q_r(a)$	=	$\int \tau_{rz}(a, z) \, \mathrm{d}A$

(14)

It may be noted that the linear plate theory does not permit us to match the deflections at all points along the interface. We would expect that the accuracy of the solution will improve for thinner plates and some estimate of the accuracy may be obtained by examining the displacement match across the interface. The stress distribution in the interior of the plate will improve in accuracy as we move away from the interface by Saint Venant's Principle.

The governing differential equation for the deflection of isotropic, homogeneous plates is

$$D\nabla^4 w(r) = q(r) \tag{15}$$

where

$$D = \frac{2}{3}\frac{Eb^3}{(1-\nu^2)}.$$

The shear and moment distributions are related to the deflection in the following manner

$$Q_r = -D\frac{\mathrm{d}}{\mathrm{d}r}\nabla^2 w \tag{16}$$

$$M_r = -D\left[w_{rr} + \nu\frac{1}{r}w_r\right] \tag{17}$$

Summing forces in the z direction to obtain shear at $r = \beta$, yields

$$Q_\beta \beta + \int_0^\beta q(\rho)\rho \, \mathrm{d}\rho = 0$$

$$Q_\beta = -\frac{1}{\beta}\int_0^\beta \rho q(\rho) \, \mathrm{d}\rho$$

Using equation (16)

$$D\frac{\mathrm{d}}{\mathrm{d}\beta}\left[\frac{1}{\beta}\frac{\mathrm{d}}{\mathrm{d}\beta}\left(\beta\frac{\mathrm{d}w(\beta)}{\mathrm{d}\beta}\right)\right] = \frac{1}{\beta}\int_0^\beta \rho q(\rho)\,\mathrm{d}\rho$$

Assuming that the necessary functions are integrable over the range $0 \leq \rho \leq a$ then

$$\begin{aligned} Dw(r) &= I_1(r) + A\frac{r^2}{2} + B\ln(r) + C \\ D\frac{\mathrm{d}w(r)}{\mathrm{d}r} &= I_2(r) + Ar + B\frac{1}{r} \end{aligned} \tag{18}$$

where

$$\begin{aligned} I_1(r) &= \int_0^r \frac{1}{\gamma}\int_0^\gamma \delta\int_0^\delta \frac{1}{\beta}\int_0^\beta \rho q(\rho)\,\mathrm{d}\rho\,\mathrm{d}\beta\,\mathrm{d}\delta\,\mathrm{d}\gamma \\ I_2(r) &= \frac{1}{r}\int_0^r \delta\int_0^\delta \frac{1}{\beta}\int_0^\beta \rho q(\rho)\,\mathrm{d}\rho\,\mathrm{d}\beta\,\mathrm{d}\delta \end{aligned}$$

Conditions (14) are applied to specify quantities A, C, S, T. Bounded solutions at the origin imply $B = 0$. Condition (14a) yields

$$I_1(a) + A\frac{a^2}{2} + C = \frac{D}{G}[S\{ws(a, 0)\} + T\{wt(a, 0)\}]. \tag{19}$$

Condition (14b) yields

$$I_2(a) + Aa + \frac{-D}{G}[S\{uzs(a, 0)\} + T\{uzt(a, 0)\}]. \tag{20}$$

Condition (14c) yields

$$(1-\nu)\frac{I_2(a)}{a} - (1+\nu)A - I_3(a) = \frac{2}{3}b^3S \tag{21}$$

where

$$I_3(r) = \int_0^r \frac{1}{\beta}\int_0^\beta \rho q(\rho)\,\mathrm{d}\rho\,\mathrm{d}\beta.$$

Condition (14d) yields T explicitly.

$$T = \frac{-3}{4ab}\int_0^a rq(r)\,\mathrm{d}r \tag{22}$$

Equations (20) and (21) may be solved for S and A explicitly.

$$S = \frac{[2I_2(a) - aI_3(a)] + \frac{D}{G}(1+v)T\{uzt(a,0)\}}{\frac{2}{3}ab^3 - \frac{D}{G}(1+v)\{uzs(a,0)\}} \tag{23}$$

$$A = \frac{-\left[\frac{D}{G}\frac{(1-v)}{a}\{uzs(a,0)\} + \frac{2}{3}b^3\right]I_2(a) + \frac{D}{G}\left[\{uzs(a,0)\}I_3(a) + \frac{2}{3}b^3 T\{uzt(a,0)\}\right]}{\frac{2}{3}ab^3 - \frac{D}{G}(1+v)\{uzs(a,0)\}} \tag{24}$$

Equation (19) yields C

$$C = \frac{D}{G}[S\{ws(a,0)\} + T\{wt(a,0)\}] - A\frac{a^2}{2} - I_1(a) \tag{25}$$

4. ILLUSTRATIVE EXAMPLE

Further investigation would be awkward to carry out in general. The remaining text will deal with specific loading, geometry and material parameters.

Let $q(r) = q$, a constant. The load q for constant loading may be considered as a multiplying factor in the expressions for $w(r)$ and in this case is set at 1·0 for all numerical results.

For purposes of illustration, three plate geometries will be used. Two are well within the bounds of thin plate theory and will have thickness to diameter ratios of 0·02 and 0·05. The last will assume this ratio to be 0·10 where it is recognized that thin plate theory may not be a good model for this case. For each of these ratios, eight ratios of elastic moduli of the plate and wall will be used. This ratio E_p/E_W, will range from 0 to 10 where 0 will represent the plate built into an inflexible wall and the present development reduces to the classical solution for a clamped plate. A value of $E_p/E_W = \infty$ does not exactly correspond to a simply supported plate. In order to reduce the general result to the simply supported case it is also necessary that terms involving T, maximum shear stress at the wall, be negligible compared to other surviving terms.

Each of the cases will be computed for a Poisson's ratio of $v = 0{\cdot}25$ in both the wall and the plate, and also for $v = 0{\cdot}3$ in both wall and plate, although this development does allow values of v in the plate to differ from those in the wall.

Deflections $w(r)$ of the mid-plane of the plate, together with corresponding maximum stresses S and T at the wall, are displayed in Fig. 1.

For the particular loading $q(r) = q$, a constant, the maximum deflection of a clamped plate is $w_c = qa^4/64D$ and for a simply supported plate is $w_s = [(5+v)/(1+v)]qa^4/64D$. The Ratio $R_1 = w_s/w_c = 4{\cdot}2$ and 4·08 for $v = 0{\cdot}25$ and $v = 0{\cdot}3$ respectively. A corresponding ratio R_2 for the deflections in Fig. 1 can be devised by subtracting the deflection of the wall from the total deflection leaving only that due to deformation of the plate.

$$R_2 = [w_{10}(0) - w_{10}(a)]/w_0(0)$$

where $w_{10}(r)$ is that deflection for $E_p/E_W = 10$ and $w_0(0) \equiv w_c$ is the deflection for $E_p/E_W = 0$.

For the plates represented in Fig. 1, $3{\cdot}9 < R_2 < 4{\cdot}2$ therefore one might conclude that the deformation of the plate as $E_p/E_W \to \infty$ is similar to a simply supported plate. Larger

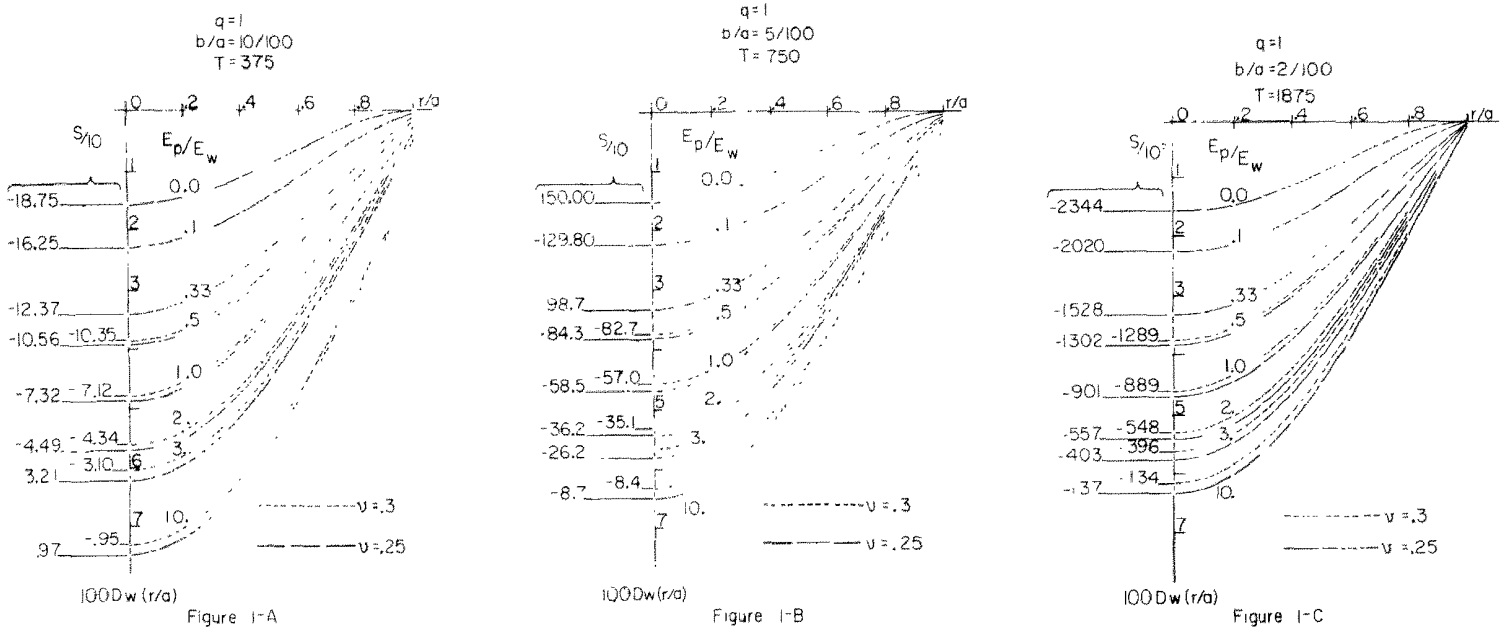

FIG. 1. Plate displacements and the associated maximum stresses (S and T) at the interface between the plate and solid for the illustrative example.

deflections are allowed mainly as a result of smaller restraint against rotation. It would seem that the contribution of terms involving T, shear stress at the wall, is small, however it must be remembered that T terms also increase the slope at the wall as well as the vertical deflection. If the load distribution was moved toward the wall instead of being uniformly distributed these terms would be much more significant.

It is apparent that for each of these thickness/diameter ratios, the deflections $w(r)$ based on an assumption of a rigid wall compared with deflections when using a wall and plate of the same material, never differ by less than 200% for any given r. Similarly, the maximum radial tensile stress S at the wall never varies by less than 200%. From a practical viewpoint, a stress analysis based on the rigid wall assumption is on the safe side. The effect of Poisson's ratio varying from 0·25 to 0·30 is relatively small but becomes more significant for thinner plates.

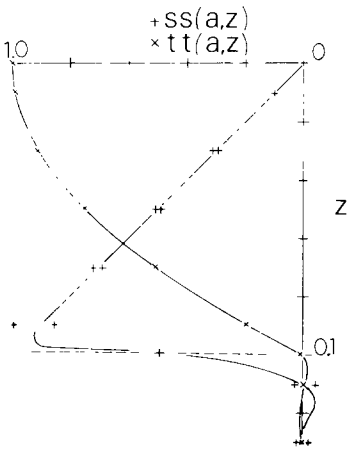

FIG. 2. Resultant stress profiles for unit S and T applied to the elastic solid.

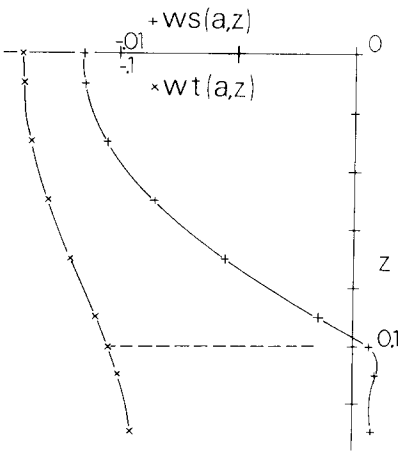

FIG. 3. Displacements of the surface of the elastic solid in the z-direction associated with applied stress in Fig. 2.

As expected, the deflection at the wall is small for thinner plates, while rotation at the wall is still comparatively large.

There is little reason to believe that the trends indicated by this example would change significantly for other usual loadings and geometries within the scope of the problem.

Also of interest is the behavior of the wall, particularly at the interface between the wall and plate. The integral quantities of (12) or (13) represent the various displacements and slopes due to a unit load S or T. The results of computation for the case where $b/a = \frac{1}{10}$, $\nu = 0{\cdot}25$ are displayed in Figs. 2–5. Decay of the solutions with increasing r values was explored only for $w(r, 0)$ and the results are given in Fig. 6.

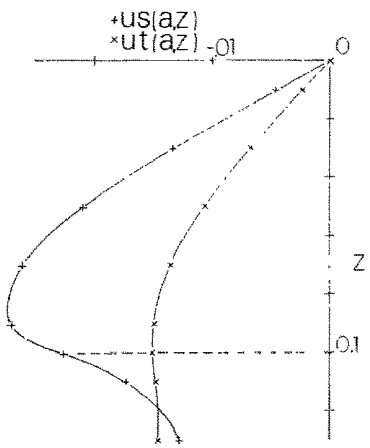

FIG. 4. Displacements of the surface of the elastic solid in the r-direction associated with applied stress in Fig. 2.

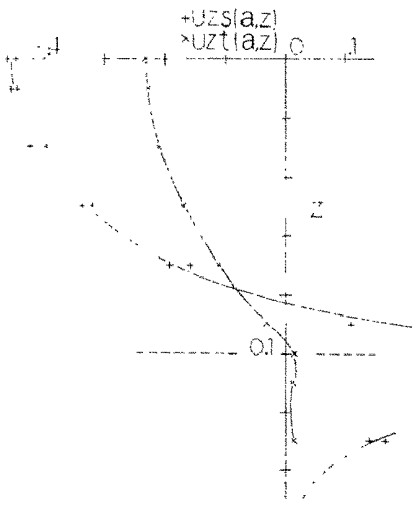

FIG. 5. Slopes associated with Fig. 4.

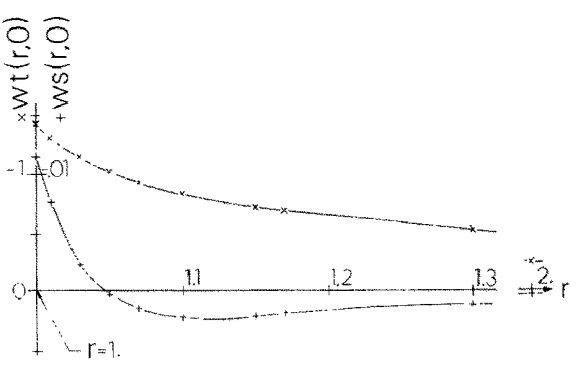

FIG. 6. Displacements in the z-direction of the plane $z = 0$ in the elastic solid associated with applied stress in Fig. 2.

Acknowledgement—The authors wish to acknowledge helpful suggestions given by Dr. J. S. Frame, Professor of Mathematics at Michigan State University and those given by Dr. I. N. Sneddon, Professor of Mathematics at the University of Glasgow, Scotland.

REFERENCES

[1] C. WEBER, The deflection of loaded gears and the effect on their load carrying capacity. Department of Scientific and Industrial Research, Sponsored Research, Germany. Report No. 3, Part 1, England (1949).
[2] N. I. MUSKHELISHVILI, *Some Basic Problems of the Mathematical Theory of Elasticity*, 3rd edition, p. 471. Noordhoff (1953).
[3] W. J. O'DONNELL. The additional deflection of a cantilever due to the elasticity of the support. *J. appl. Mech.* **27**, 461–464 (1960).
[4] R. D. COOK. Deflections of a series of cantilevers due to elasticity of support. *J. appl. Mech.* **34**, 760–761 (1967).
[5] J. M. BROWN and A. S. HALL. Bending of a circular shaft terminating in a semi-infinite body. *J. appl. Mech.* **29**, 86–90 (1962).
[6] O. L. BOWIE. Elastic stresses due to a semi-infinite band of hydrostatic pressure acting over a cylindrical hole in an infinite solid. *Q. appl. Math.* **5**, 100 (1947).
[7] C. J. TRANTER, On the elastic distortion of a cylindrical hole by a localized hydrostatic pressure. *Q. appl. Math.* **4**, 298–302 (1946).
[8] S. C. DAS, On the elastic distortion of a cylindrical hole by localized axial shears on the inner boundary. *Ind. J. theor. Phys.* **1**, 41–46 (1953).
[9] K. A. BLENKARN and J. C. WILHOIT, Stresses due to a band of normal stress at the entrance of a circular hole. *J. appl. Mech.* **29**, 647–650 (1962).
[10] J. S. FRAME, *Numerical Integration and the Euler–MacLauren Summation Formula*. Michigan State University (1967).

(*Received* 17 *October* 1968; *revised* 12 *May* 1969)

Абстракт—Решается задача, касающаяся круглого диска или пластинки, прикрепленных к стенке цилиндрического отверстия в бесконечном теле. Распределение напряжений между двумя граничными поверхностями сравниваются с обыкновенной теорией пластинок. Угол наклона и перемещения подходят близи стенки, где серединная поверхность пластинки пересекает неограниуенное тело. Задача решается для любого случая осесииметрической нагрузки пластинки, одномерной толщины и параметров материала. Метод можно также применить к другому любому осесимметрическому решению пластинки без учета сил в серединной поверхности. Параметры материала в пластинке и в поддерживающем теле можно определитв независимо. Для особых случаев, прогибы пластинки при предложении жесткой стенки, как и в противопололожности при предположении такого же самого материала пластинки и стенки никогда не разнятся менее, чем на 200%. Решение указывает на то, что результаты полученные при исследованиях, моглибы значительно изменится для случаев других обыкновенных нагрузок и геометрий, в рамках рассматриваемой задачи.